Prediction and Observation of Sustained Oscillations in a Sheared Liquid Crystalline Polymer

M. Grosso and S. Crescitelli
Dipartimento di Ingegneria Chimica, Universitá Federico II di Napoli, Piazzale Tecchio 80, I-80125, Napoli, Italia

E. Somma, J. Vermant, and P. Moldenaers
Department of Chemical Engineering, Katholieke Universiteit Leuven, W. de Croylaan 46, B-3001 Leuven, Belgium

P. L. Maffettone*
Dipartimento di Scienza dei Materiali ed Ingegneria Chimica, Politecnico di Torino, Corso Duca degli Abruzzi 24, I-10129, Torino, Italia

(Received 9 December 2002; published 5 March 2003)

Experimental observations of sustained oscillations of both shear stress and first normal stress differences are reported in flowing liquid crystalline polymers in a limited range of shear rates. The results can be described by considering the response of a rigid-rod model. Depending on the initial conditions, the frequency spectrum of the stress signal contains either one or two characteristic frequencies. This can be explained by the occurrence of either pure "wagging" or the coexistence of wagging and "log-rolling" behavior of the director.

DOI: 10.1103/PhysRevLett.90.098304 PACS numbers: 83.80.Xz, 05.45.Tp, 83.10.–y, 83.85.Cg

Nematic phases show several peculiar rheological features that are due to both intrinsic anisotropy of the molecules and spatial variation of an average molecular orientation (the so-called *director*) in the bulk. When dealing with polymers in the nematic phase, the long relaxation times typical of polymeric systems add complexity as the flow field can easily distort the equilibrium orientational molecular configuration.

We here present the experimental establishment of the existence of a periodic response under constant shear flow in a narrow region of shear rates. The experiments are also confirmed by the predictions of a well known microscopic model, i.e., the rigid-rod model by Doi and Hess [1,2].

The system under investigation is a solution of poly-γ-(benzylglutamate) (molecular weight of 345.000, *L*-enantiomer, Sigma Chemical Co.) in *m*-cresol (12% by weight). The rheology and microstructure of similar systems have been studied extensively in the past [3–6]. The nematic phase is supposed to be a tumbling nematic at low shear rates, i.e., the average orientation rotates indefinitely in time under constant shear rate, whereas at large shear rates a flow-aligning behavior is recovered [7]. In a region of intermediate shear rates different oscillatory regimes can be attained [8–10]. The material and the measurement conditions were chosen in such a manner that the transition to flow-aligning occurs at the lowest possible shear rates to avoid the need for too fast measurements of the stress signals. For the same reason, the temperature has been kept low to shift the transition to still lower shear rates [6,11].

The stress response was measured using a strain controlled rheometer (ARES, Rheometric Scientific, Piscataway, NJ). Whereas the instrument makes it possible to measure fast transients, even for normal stresses, the data-acquisition system provided by the manufacturer allows only a limited number of data points to be collected. To obtain larger data sets as required to analyze the signal in the frequency domain, the analog force and torque signals were fed into a signal conditioner (Stanford Research Systems) connected to a 12-bit data-acquisition device (PCI-6033 from National Instruments, using Labview), which also allowed better time resolutions (0.01 s). The temperature was kept at $10.0 \pm 0.1\,^{\circ}\mathrm{C}$ by means of a circulating fluid bath. Cone-and-plate geometry ($D = 25$ mm and cone angle 0.1 rad) was used throughout to ensure a homogeneous shear rate in the sample. Under these conditions the transition of positive to negative normal stresses occurred at $2\ \mathrm{s}^{-1}$.

Liquid crystalline polymers typically display a long lived and complex polydomain texture [12,13]. Reproducible and well defined initial conditions can be created by well defined flows. Two different flow histories have been imposed: flow-reversal experiments, where only the flow direction is reversed at a constant shear rate in the oscillatory regime, and step-down experiments, where sudden decrease of the shear rate from the flow aligning to the oscillatory regime is imposed.

Figure 1 shows the long time behavior of the shear stress, σ_{12}, and the corresponding power spectrum after the flow direction has been reversed. The spectrum was calculated using a discrete Fourier transform algorithm. Note that the frequency (ω) has been made dimensionless with the shear rate. Figures 1(a) and 1(b) show that the response at $1\ \mathrm{s}^{-1}$ is essentially stationary, without any periodicity. The sustained oscillatory response found in the intermediate shear rate range shown in Fig. 1(c) was found to be reproducible and stable over time: the

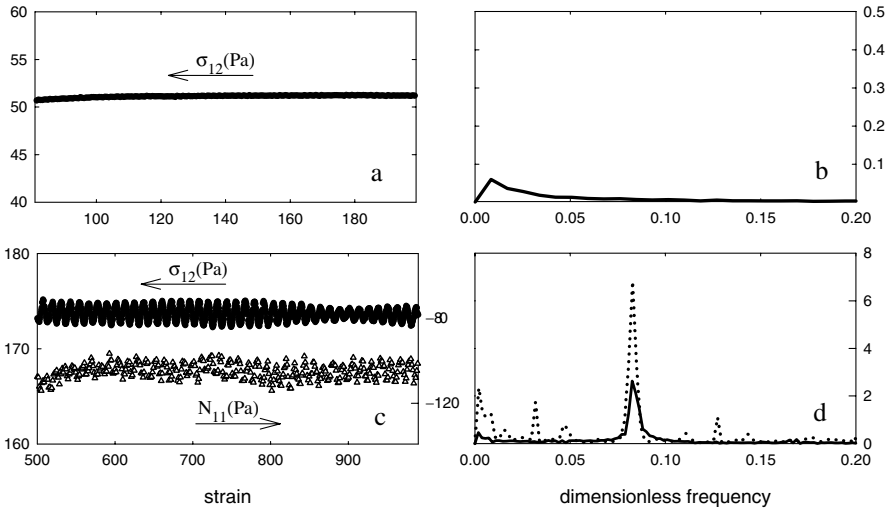

FIG. 1. The shear stress vs strain and the corresponding power spectra after flow reversal. (a),(b) $\dot{\gamma} = 1\ s^{-1}$; (c),(d) $\dot{\gamma} = 7\ s^{-1}$. In (c) the circles represent the shear stress and the triangles the first normal stress difference. In (d) the solid line is the shear stress power spectrum, and the dotted line is the normal stress power spectrum.

oscillations persist up to 1000 strain units. The dimensionless characteristic frequency in Fig. 1(d) is clearly visible in the spectrum at 0.083. It should be noted that the rotation of the motor of the rheometer has a dimensionless frequency of 0.018, thus significantly lower than the observed frequency.

Similar features are observed for the first normal stress difference, N_{11}, shown in Fig. 1(c). The data, however, are noisier in this case as apparent in the power spectrum in Fig. 1(d). It should be noted that the characteristic frequency coincides with that found in the shear stress data. A complete report on the experiments will be presented elsewhere.

In a second set of experiments, step-down experiments from the flow-aligning regime were performed. The initial shear rate of 30 s^{-1} was chosen to be well within this regime. Data on the stress evolution after decreasing the shear rate to 7 s^{-1} are shown in Fig. 2(a). The corresponding power spectrum obtained by analyzing over more than 400 strain units of the stress response is shown in Fig. 2(b). Again, a periodic response is found, but in this case two distinct peaks can be seen in the spectrum of Fig. 2(b). The frequency of the motor motion is again visible at lower frequencies (0.018). The major peak at $\omega = 0.083$ corresponds to the one found in the flow-reversal experiments. The minor peak is found at $\omega = 0.076$. Similar results are found for the first normal stress difference dynamics and also at other shear rates. The sustained oscillatory response was observed only in a narrow shear rate window, between 5 and 15 s^{-1}.

The experimental data can be quantitatively compared to the predictions of the rigid-rod model [1,2]. The rheology in the nematic phases has been widely and successfully studied in the last decades with that approach. The model is capable of describing the stress response at intermediate and high shear rates when spatial distortion effects can be neglected [8,9,14], i.e., when the flow is strong enough to destroy textures. The nematogenic molecules are treated as rigid rods, and the sample is described with an orientational distribution function. Its evolution is predicted with a continuity equation for the

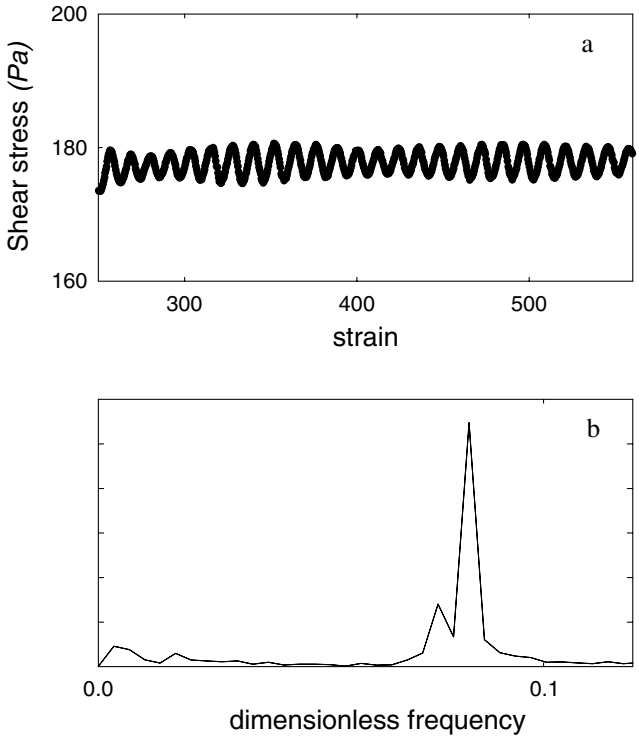

FIG. 2. The shear stress vs the strain (a) and the corresponding power spectrum (b) after a step-down from 30 s^{-1} to $\dot{\gamma} = 7\ s^{-1}$.

distribution function (a Fokker-Planck equation) that accounts for thermal agitation, excluded volume effects, and macroscopic flow. In dimensionless terms the equation is

$$\frac{\partial \psi}{\partial t} = \frac{\partial}{\partial \mathbf{u}} \cdot \left[\frac{\partial \psi}{\partial \mathbf{u}} + \frac{\psi}{k_B T} \frac{\partial V(\mathbf{u})}{\partial \mathbf{u}} - (\mathbf{K} \cdot \mathbf{u} - \mathbf{uuu}:\mathbf{K})\psi \right]. \quad (1)$$

In Eq. (1), t is time made dimensionless with an average rotational diffusivity (not appearing in the equation), $k_B T$ is the Boltzmann factor, $V(\mathbf{u})$ represents a mean field nematic potential, and $\mathbf{K}$ is the dimensionless velocity gradient. The partial derivative with respect to $\mathbf{u}$ represents the gradient over the unit sphere. It should be noted that Eq. (1) assumes constant rotational diffusivity and rods with infinite aspect ratio. The nematic potential considered here is the Maier-Saupe [15] one,

$$V(\mathbf{u}) = -\tfrac{3}{2} U k_B T \langle \mathbf{uu} \rangle : \mathbf{uu}, \quad (2)$$

where the brackets imply ensemble average. In Eq. (2), $U = \nu d L^2$ is the intensity of the nematic field, where d is the rod diameter, L is the length, and ν is the number of molecules per unit of volume. A stable nematic phase coexists at rest with the isotropic solution for $U_{\mathrm{tr}} = 4.49 \leq U \leq 5$, while for $U \geq 5$ the only stable solution is the nematic one [10].

In Eq. (1) the shear rate G, made dimensionless through the rotational diffusivity, is contained in the velocity gradient. The velocity of the shear flow considered here is given by $\mathbf{v} = [Gz, 0, 0]$; thus, x is the flow direction, y is the vorticity direction, and z is the velocity gradient direction. In the following, the plane xz will be referred to as the shear plane.

The stress tensor can be calculated once the orientation distribution function is known, as was derived by Doi and Edwards [16]. The model predicts the rodlike polymers to be tumbling nematic at low shear rates for $U \geq 5$: in the texture-free assumption, the average orientation does not achieve a steady state; rather, it rotates indefinitely in time. The polymeric nature, however, adds several nonlinear features. For example, at large shear rates the periodic response is suppressed, and the system becomes flow aligning, that is, the system is predicted to reach a steady state with the average orientation within the shearing plane. This feature and the stress response under these flow conditions have been confirmed by experimental results, e.g., [14]. In the following, only the elastic contribution to the total stress will be calculated.

In the intermediate shear rate region, the model predictions become much more complex. Larson [8] and Marrucci and Maffettone [9] found a periodic solution, which was named *wagging regime* by Larson: the director oscillates in the shear plane between two limiting angles. Stable stationary solutions with the director aligned along the vorticity axis were also found [8], and that regime was named *log-rolling*. Subsequent analysis performed with continuation algorithms revealed the existence of multiplicity [10].

The model predictions have actually been used for guidance in the experimental quest of periodic regimes. To this end, the change in the sign of the first normal stress difference usually identifies the transitions between the different regimes of director dynamics. The wagging and log-rolling solutions are expected to occur in a region, around the shear rate where the first normal stress difference is at its most negative value [8,10]. For the sample under investigation this occurs at 10 s^{-1} at 10 °C.

The intensity of the nematic potential was estimated by considering that $U/U_{\mathrm{tr}} = C/C_{\mathrm{tr}}$, where the indices tr denote the transition value ($U_{\mathrm{tr}} = 4.49$, $C = 12\%$, $C_{\mathrm{tr}} = 8.2\%$ [17]). Consequently, a reasonable value of U was chosen as $U = 6.66$. In order to compare with experiments, a shear rate range close to the flow-aligning regime was selected. For $U = 6.66$ this range of shear rates (9.5–16.15) is characterized by the coexistence of a stable wagging regime with a stable *log-rolling* solution (see Fig. 7 in [10]). Figure 3 shows the spectrum of the simulated shear stress signal in the wagging regime calculated with $U = 6.66$ and $G = 14.0$. The signal was determined by choosing a strain sampling equal to that used in the experiments. It can be noted that the results do not quantitatively change in this range of shear rate values. The characteristic dimensionless frequency ($\omega = 0.076$) is very close to the value ($\omega = 0.083$) that was experimentally obtained in the flow-reversal experiments. Thus, it can be concluded that the experimental oscillating response at intermediate shear rate corresponds to the so-called wagging regime.

A tentative explanation of the double peak scenario found in step-down experiments [Fig. 2(b)] is proposed here based on the hypothesis that some of the multiple regimes predicted by the model at intermediate shear rates can actually coexist during flow. The sample is

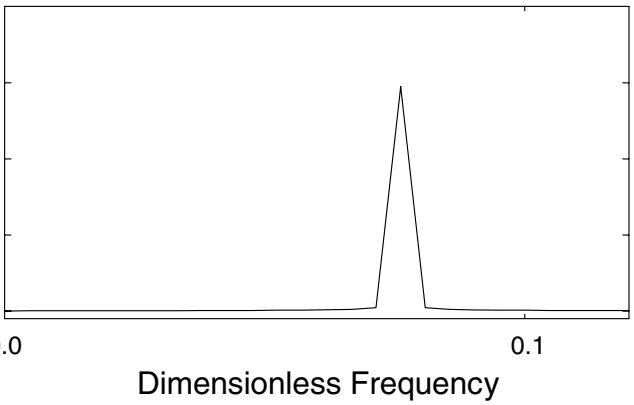

FIG. 3. The power spectrum of the wagging solution as a function of the dimensionless frequency as predicted by the rigid rod model for $U = 6.66$ and $G = 14$.

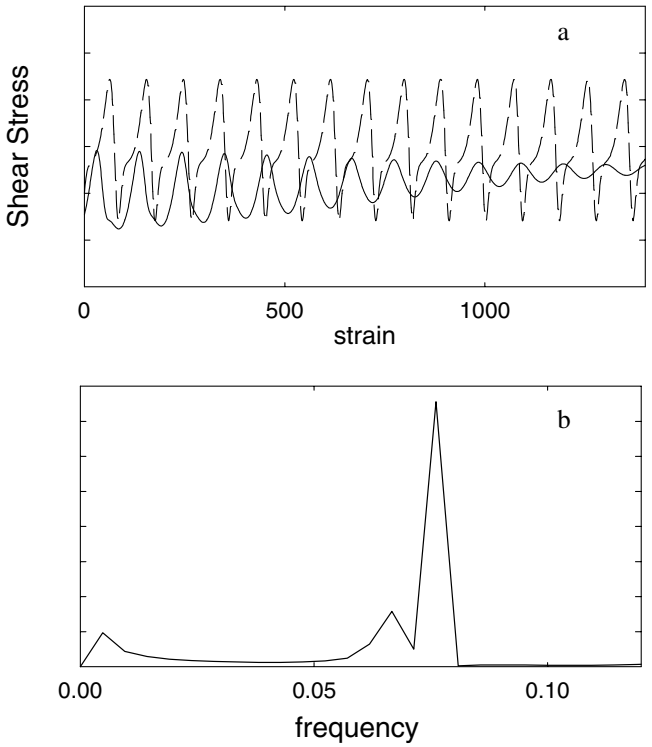

FIG. 4. (a) The shear stress predicted with the rigid-rod model for $U = 6.66$ and $G = 14$ for two different initial director orientations. The dashed line represents the wagging response, and the solid line corresponds to the response of a domain tending to log-rolling. (b) The power spectrum obtained by adding the above stress signals with 90% wagging and 10% log-rolling.

assumed to consist of several domains, and it is suggested that they may attain different asymptotic regimes. A generic domain is supposed to evolve independently from all others as the hydrodynamic stresses dominate the ones associated with distortions of the director field, and the total stress is determined as a linear combination of the contribution of each domain. The initial conditions, created in the case of step-down from the flow-aligning regime experiments, are such that the sample is aligned in the shearing plane. When stepping down the shear rate, different regions will tend to wag while a small fraction of domains that are created could be attracted to the log-rolling state. This attraction towards the log-rolling state is less likely to occur for the case of the flow-reversal experiments, as the dynamics states before and after flow reversal will be essentially the same. Thus, it is conceivable that the log-rolling domains, when present, will remain essentially unchanged upon reversal, and the wagging domains will quickly flip within the shearing plane to continue their oscillations around the new imposed direction.

The step-down experiments were described numerically assuming that the stress is composed of contributions of domains remaining in the shear plane with a small fraction of domains evolving towards the vorticity. Figure 4(a) reports, as an example, the time evolution of the stress for two domains having different initial conditions: one evolving towards the wagging regime, the other tending to the log-rolling solution. The evolution towards log-rolling is characterized by a very long (up to $\sim$1500 strain units) damped oscillating transient. This transient is characterized by a frequency different from that of the wagging regime. One can combine the two signals predicted during the transient by suitably weighting the two contributions. Figure 4(b) shows the corresponding power spectrum obtained when the wagging domains constitute 90% of the sample. The weight is the only adjustable parameter required to adequately describe the experimental results. The frequencies of the two peaks in the spectrum are very close to those obtained experimentally in Fig. 2. The peak at $\omega = 0.067$ visible in Fig. 4(b) is due to the transient of the domains tending to log-rolling.

In conclusion, clear experimental results for sustained wagging dynamics have been presented and supported by the Doi-Hess model. In experiments where the flow is stepped down from the flow aligning into the wagging regime, a coexistence between wagging and log-rolling is revealed.

The financial support of the EU through INTAS Project No. 00-00278 is gratefully acknowledged.

*Electronic address: pier.luca.maffettone@polito.it

[1] S. Hess, Z. Naturforsch. A **31**, 1034 (1976).
[2] M. Doi, J. Polym. Sci. Polym. Phys. Ed. **19**, 229 (1981).
[3] P. Moldenaers and J. Mewis, J. Rheol. **30**, 567 (1986).
[4] J. Mewis and P. Moldenaers, Mol. Cryst. Liq. Cryst. **153**, 291 (1987).
[5] P. L. Maffettone *et al.*, J. Chem. Phys. **100**, 7736 (1994).
[6] J. Mewis *et al.*, Macromolecules **30**, 1323 (1997).
[7] G. Marrucci and F. Greco, *Advances in Chemical Physics*, edited by I. Prigogine and S. Rice (Wiley, New York, 1993), Vol. 86, p. 331.
[8] R. G. Larson, Macromolecules **23**, 3983 (1990).
[9] G. Marrucci and P. L. Maffettone, Macromolecules **22**, 4076 (1989).
[10] V. Faraoni *et al.*, J. Rheol. **43**, 829 (1999).
[11] J. Mewis and P. Moldenaers, Chem. Eng. Commun. **53**, 33 (1987).
[12] R. G. Larson and D. W. Mead, Liq. Cryst. **15**, 151 (1993).
[13] J. Vermant *et al.*, J. Non-Newtonian Fluid Mech. **53**, 1 (1994).
[14] W. R. Burghardt, Macromol. Chem. Phys. **199**, 471 (1998).
[15] W. Maier and A. Z. Saupe, Naturforsch. A **14**, 882 (1959).
[16] M. Doi and S. F. Edwards, *The Theory of Polymer Dynamics* (Clarendon, Oxford, 1986).
[17] J. Hermans, J. Colloid Sci. **17**, 638 (1962).